Reduced damping of surface plasmons at low temperatures

Mingzhao Liu (刘铭钊),[1,2,*] Matthew Pelton,[2] and Philippe Guyot-Sionnest[1,†]
[1]*James Franck Institute, The University of Chicago, Chicago, Illinois 60637, USA*
[2]*Center for Nanoscale Materials, Argonne National Laboratory, Argonne, Illinois 60439, USA*
(Received 9 October 2008; revised manuscript received 7 December 2008; published 27 January 2009)

We investigated the effectiveness of low temperatures in reducing plasmon damping by measuring the homogeneous linewidth of plasmon resonances (~1.5 eV) in nanoscale gold bipyramids at temperatures from 293 to 6 K. The linewidth drops linearly with temperature and approaches a constant value at approximately 50 K. Measurements were performed on monodisperse ensembles as well as on single particles. The 30% decrease in the homogeneous linewidth with decreasing temperature is well accounted for by the reduced electron-phonon scattering. The other relaxation mechanisms—electron-electron scattering, electron-surface scattering, and radiative relaxation—do not change significantly with temperature.

DOI: 10.1103/PhysRevB.79.035418 PACS number(s): 78.67.Bf

I. INTRODUCTION

Metal structures are routinely used to receive, transmit, and broadcast radiation at radiowave and microwave frequencies, where they behave as nearly perfect conductors. In recent years, there has been significant effort to extend this functionality to the optical regime by scaling components down to the nanometer scale, giving birth to the field of plasmonics.[1] The interaction between light and surface plasmons in metal nanostructures has the potential to enable a wide variety of applications, including emission enhancement,[2,3] waveguiding below the diffraction limit,[4] negative refraction,[5,6] and biochemical sensing.[7] Practical realizations, though, are often limited by strong damping.[8] For a perfect bulk metal crystal, these losses are mainly due to electron-phonon and electron-electron scatterings. In direct-current measurements, metallic conductivity improves by orders of magnitude upon cooling to liquid-helium temperature,[9] and the near-infrared (IR) reflectivity of noble-metal films also increases at low temperature.[10] It is therefore interesting to investigate the effect of temperature on the damping of plasmons in metal nanostructures. In particular, the relaxation rate, $\gamma(\omega)$, for a localized plasmon resonance at frequency ω is simply given by the spectral linewidth $\Gamma(\omega)$ of the plasmon resonance, which is readily measured experimentally.[11]

Kreibig[12] studied the temperature dependence of the plasmon linewidth for spherical silver nanoparticles embedded in glass. However, the observed linewidth reduction was not significant partly because the spherical-particle resonance is around 3 eV and is thus dominated by strong electronic transitions between the *d* and *sp* bands of silver. Recent advances in the synthesis of metal nanoparticles with controlled size and shape allow the plasmon resonance to be tuned away from interband transitions, overcoming this limitation. In particular, gold-bipyramid colloids[13] have a sharp longitudinal-plasmon resonance that can be tuned around 1.5 eV, which is far away from the interband transition at 2.5 eV. Unlike lithographically defined nanostructures, these particles are free of surface roughness, allowing intrinsic damping mechanisms to be investigated. Moreover, they can be synthesized with high uniformity in size and shape, so that the effects of inhomogeneous broadening on the plasmon linewidths are small, and homogeneous linewidths can be inferred even from measurements on large ensembles. The gold bipyramids thus present a unique opportunity to investigate the fundamental mechanisms that determine the temperature-dependent damping of plasmons in metal nanostructures.

II. EXPERIMENTAL

A. Ensemble measurement

The gold bipyramids have a pentagonal bipyramidal shape and are highly monodisperse in size and shape, with a length of approximately 90 nm and diameter of 30 nm. The gold nanoparticles were deposited on a plain glass substrate to form a sparse monolayer using a polyelectrolyte approach developed by Gole and Murphy.[14] After the coating, part of the glass slide was wiped by a cotton swab to remove the gold nanoparticles so that this area can be used as a reference for the absorption spectrum. Another piece of glass slide was then glued on top of the specimen using a transparent epoxy, which gave the gold bipyramid a nearly homogeneous dielectric environment with a refractive index of 1.5. The optical density of the sample was moderate (~0.1) to limit plasmon coupling between adjacent nanoparticles. The substrate was held vertically in a cryostat cooled by liquid helium. Spectra taken at different temperatures are shown in Fig. 1(a). The linewidth [full width at half maximum (FWHM)] is plotted against the temperature in Fig. 1(b).

We note that the optical density of the film also increases as it is cooled down. Interestingly, the area under the absorption curve increases with decreased temperature; however, as noted by Kreibig and Vollmer,[15] the integrated oscillator strength should be constant within the narrow frequency range considered. The apparent discrepancy arises because the measured extinction spectra include a contribution of approximately 20% from scattering, as shown by numerical simulations.[16] Unlike the oscillator strength, which remains constant, the integrated resonant scattering amplitude increases as $1/\Gamma$, according to the optical theorem.[17]

Even in this highly monodisperse sample, the linewidth is still inhomogeneously broadened. Assuming that the inho-

 ©2009 The American Physical Society

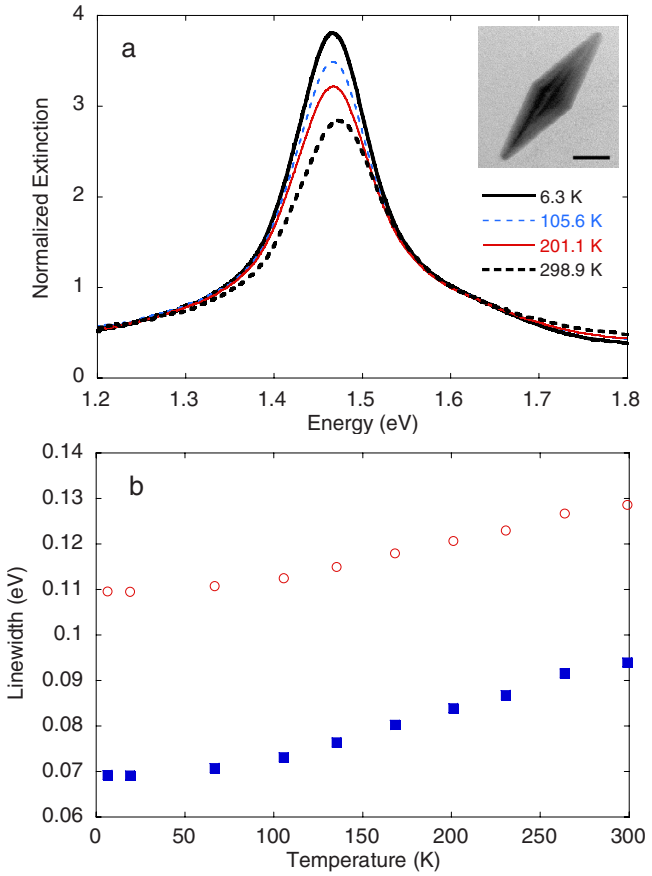

FIG. 1. (Color online) (a) Longitudinal-plasmon resonance of a monolayer of gold bipyramids at different temperatures. Inset: transmission electron micrograph of a gold bipyramid (scale bar =25 nm). (b) Temperature dependence of the longitudinal-plasmon linewidth (FWHM) for the gold-bipyramid monolayer (red open circles). Knowing that the homogeneous linewidth at room temperature is 94 meV, it is possible to remove the temperature-independent inhomogeneous broadening due to the size and shape distributions, leaving the pure homogeneous linewidth (blue squares).

mogeneous broadening is independent of temperature, it can be removed from the experimental data to yield the homogeneous linewidth. If we treat the inhomogeneous spectrum as a normal distribution of Lorentzians of frequencies ω_c,

$$f(\omega_c) = \frac{1}{\sigma\sqrt{2\pi}} \exp\left[-\frac{(\omega_c - \omega_0)^2}{2\sigma^2}\right], \tag{1}$$

where ω_0 is the expectation value for ω_c, σ is the standard deviation, and all Lorentzians have the same width Γ, i.e.,

$$s(\omega, \omega_c) = \frac{A\Gamma}{4(\omega - \omega_c)^2 + \Gamma^2}, \tag{2}$$

then the ensemble spectrum is given by a Voigt profile

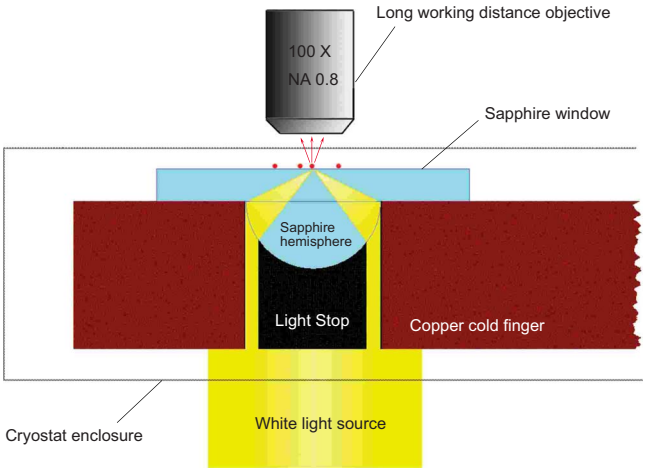

FIG. 2. (Color online) Experimental setup for low-temperature dark-field microscopy. The dark-field illumination is provided by a sapphire hemisphere with the center blocked, which gives a numerical aperture greater than 0.9. The copper cold finger is cooled by externally supplied cryogenic fluid (not shown).

$$S(\omega) = \int_{-\infty}^{\infty} f(\omega_c) s(\omega, \omega_c) d\omega_c. \tag{3}$$

The linewidth, Γ_V, of the Voigt profile is not an elementary function of σ and Γ, but a highly accurate approximation is given by Olivero and Longbothum:[18]

$$\Gamma_V = 0.5346\Gamma + \sqrt{0.2166\Gamma^2 + 8\sigma^2 \ln 2}. \tag{4}$$

At room temperature, the linewidth, Γ_V, for the gold-bipyramid monolayer is 129 meV [Fig. 1(a)]. Using the room-temperature homogeneous linewidth measured on single gold bipyramids of 94 meV,[13] the standard deviation σ is therefore determined to be 28 meV. This value can then be used to determine Γ at different temperatures, as shown in Fig. 1(b). Γ has a linear temperature dependence above 100 K, with a slope of $(1.10 \pm 0.03) \times 10^{-4}$ eV K^{-1}. Below approximately 50 K, Γ approaches a constant value of 69 meV, approximately 30% lower than the room-temperature linewidth.

B. Single-particle measurement

In order to verify the validity of the assumptions used in extracting the temperature-dependent homogeneous linewidth, we also studied the optical scattering spectra from single gold bipyramids at room temperature (298 K) and at liquid-nitrogen temperature (77 K). For this purpose, we developed a different dark-field condenser, consisting of a sapphire window, a sapphire hemisphere, and a light stop, which provided dark-field illumination with a numerical aperture greater than 0.9 (Fig. 2). The condenser was placed into a microscopy cryostat and was in good thermal contact with the cold finger. The aqueous metal colloids were transferred to a methanol solution with 1% polyvinylpyrrolidone (PVP) and drop cast onto the sapphire window. The sample was imaged using a 100× long-working-distance objective with numerical aperture of 0.8 and was illuminated by a halogen

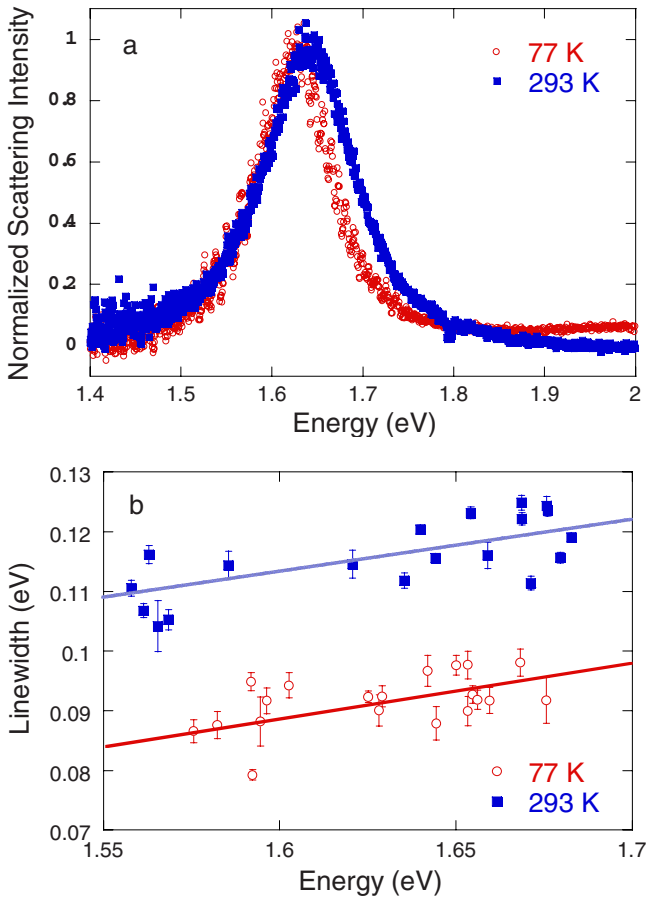

FIG. 3. (Color online) (a) Typical optical scattering spectra from single gold bipyramids taken at 293 (blue squares) and 77 K (red open circles). A clear narrowing of the resonance is seen for the lower temperature. The two spectra are representative but not from the same nanoparticle. The drift during the cooling process made it highly difficult to track the nanoparticles. (b) Measured linewidth of scattering spectra of single gold bipyramids vs their resonance energies at 293 (blue squares) and 77 K (red open circles). The lines are linear fits.

lamp through the dark-field condenser. For spectral analysis, the scattered light from each nanoparticle was focused onto the entrance slit of a grating spectrometer and was detected by a high-sensitivity back-illuminated charge coupled device (CCD) camera. At each temperature, more that 20 nanoparticles were studied. In order to achieve the best signal-to-noise ratio for the detector used, the sample was chosen to have a resonance frequency around 1.6 eV [Fig. 3(a)]. The measured homogeneous linewidths are plotted against the resonant energies in Fig. 3(b). At both temperatures, the relations follow a similar slope, consistent with previous measurements.[13] This slope is primarily due to the increasing contribution from the interband transitions at higher energies. The linewidths measured at 77 K are uniformly smaller than their room-temperature counterparts by about 24 meV, which extrapolates well to the ensemble measurement taken at 1.5 eV [Fig. 1(b)].

III. THEORETICAL MODELING

A. Relaxation mechanisms in bulk metal

Having measured the homogeneous plasmon linewidth as a function of temperature, it is possible to determine the various mechanisms responsible for plasmon damping. Electron-electron scattering was studied by Gurzhi[19] and Lawrence and Wilkins,[20] who gave the following expression for the relaxation time $\tau_{e\text{-}e}$:

$$\tau_{e\text{-}e}^{-1}(T) = \frac{\pi^3 \Sigma \Delta}{12\hbar E_F}[(k_B T)^2 + (\hbar\omega/2\pi)^2], \tag{5}$$

where E_F is the Fermi energy, Σ is the Fermi-surface average of scattering probability, and Δ is the fractional umklapp scattering. Within the temperature range explored in our measurements, the thermal energy $k_B T$ is overwhelmed by the photon energy so that the temperature dependence of electron-electron scattering is negligible. For gold at 1.47 eV, the electron-electron scattering gives a relaxation time of 19 fs, according to the measurement by Parkins *et al.*[21] Correspondingly, the electron-electron relaxation rate $\gamma_{e\text{-}e}$ is 35 meV through the relation $\gamma_{e\text{-}e} = \hbar\tau_{e\text{-}e}^{-1}$.

Electron-phonon scattering was discussed in detail by Gurzhi[22] and Holstein,[23] who treated the conduction electrons as a free electron gas with a Fermi distribution and described the phonons using a Debye model. In the absence of interband transitions, the relaxation time $\tau_{e\text{-}p}$ is given by

$$\tau_{e\text{-}p}^{-1}(T) = \tau_0^{-1}\left[\frac{2}{5} + 4\left(\frac{T}{\Theta}\right)^5 \int_0^{\Theta/T} \frac{z^4}{e^z - 1} dz\right], \tag{6}$$

where τ_0 is a constant for a given metal and Θ is the Debye temperature of this metal. This equation is derived in the limits $E_F \gg \hbar\omega \gg k_B T$ and $k_B\Theta$, where $\omega\tau_{e\text{-}p} \gg 1$, which are all satisfied for gold at 1.5 eV. For gold, the constant τ_0 is determined from its near-infrared absorption to be 30 fs, and the Debye temperature is 185 K.[10] The 2/5 term in Eq. (6) is temperature independent and reflects electron relaxation by phonon emission.

Apart from the electron-phonon scattering, there is another possible contribution to the temperature dependence, which is the dielectric constant of the medium. The dielectric constant changes slightly from room temperature to liquid-helium temperature, shifting the plasmon resonance by about 6 meV [Fig. 1(a)]. According to the linear fits in Fig. 3(b), such a shift changes the linewidth by less than 0.1 meV, which is negligible compared to the observed narrowing. Therefore we can safely rule out any effects from the medium.

The bulk electron relaxation rate of gold is the sum of both contributions,

$$\gamma = \hbar(\tau_{e\text{-}e}^{-1} + \tau_{e\text{-}p}^{-1}), \tag{7}$$

and is plotted against temperature in Fig. 4. The result is in excellent agreement with the experimental values, except that the experimental values are approximately 25 meV larger at all temperatures. This difference can be attributed to radiative damping and electron-surface scattering, as explained below.

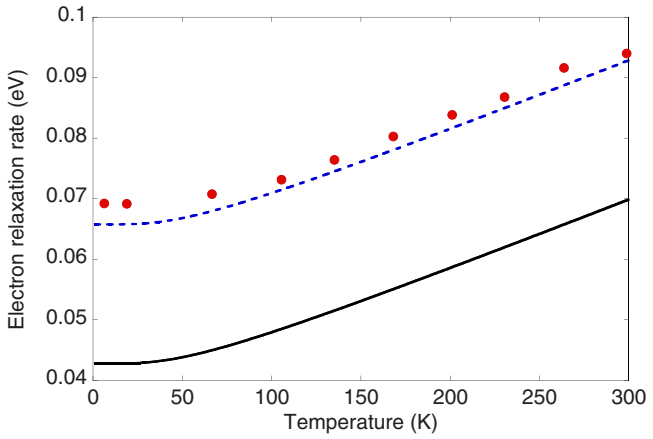

FIG. 4. (Color online) Comparison of the experimental linewidth-temperature relation to the theoretical results. The solid black line shows the temperature dependence of the bulk electron relaxation rate γ given by Eq. (7) for gold at 1.47 eV. The dashed blue line also includes the contributions from electron-surface scattering (5 meV) and radiative relaxation (18 meV). The measured homogeneous linewidths of the gold-bipyramid longitudinal-plasmon resonance are shown as red dots.

B. Radiative relaxation

Electromagnetic energy is spontaneously radiated from accelerated charges, including the oscillating conduction electrons that constitute surface plasmons. This radiative process acts as a damping term for the plasmon with the contribution $\gamma_r=\hbar\tau_r^{-1}=\hbar W^{-1}(dW)_r/dt$, where τ_r is the radiative relaxation time, $(dW)_r$ is the energy loss due to radiation, and W is the total energy of the plasmon oscillation. Without calculating the total energy W, γ_r can be evaluated by comparing with the nonradiative relaxation $\gamma_{\rm nr}$, according to the relation $\gamma_r/\gamma_{\rm nr}=(dW)_r/(dW)_{\rm nr}$, where $(dW)_{\rm nr}$ is the energy loss due to nonradiative relaxation. Within a time interval dt, the energy dissipated radiatively and nonradiatively are $\sigma_{\rm sca}Idt$ and $\sigma_{\rm abs}Idt$, respectively, where I is the incident irradiance, $\sigma_{\rm sca}$ is the scattering cross section, and $\sigma_{\rm abs}$ is the absorption cross section. The radiative relaxation rate is therefore

$$\gamma_r=\frac{\sigma_{\rm sca}}{\sigma_{\rm abs}}\gamma_{\rm nr}. \tag{8}$$

Both cross sections can be directly evaluated by finite-difference time-domain simulations,[16] which shows that $\sigma_{\rm sca}$ is about one quarter of $\sigma_{\rm abs}$ at room temperature. The radiative relaxation rate was thereby found to be approximately 18 meV at room temperature based on a nonradiative relaxation rate of 70 meV.

According to the optical theorem, the scattering and absorption cross sections are $\sigma_{\rm sca}=k^4|\alpha|^2/6\pi$ and $\sigma_{\rm abs}=k\ {\rm Im}\ \alpha$, respectively, where α is the polarizability of the nanoparticle and k is the wave number of the incident light.[17] In the quasistatic limit, the polarizability α is

$$\alpha=V\frac{\epsilon-\epsilon_m}{\epsilon+L(\epsilon-\epsilon_m)},$$

where V is the volume of the particle, ϵ_m is the dielectric constant of the medium, $\epsilon=\epsilon_1+i\epsilon_2$ is the complex dielectric constant of the particle, and L is the depolarization factor related to the shape and the orientation of the particle. At the plasmon resonance, the denominator of α is a pure imaginary number, i.e., ${\rm Re}[\epsilon_m+L(\epsilon-\epsilon_m)]=0$.

It is a good approximation to describe gold as an ideal Drude metal at near-infrared frequencies. Thus, at the plasmon resonance, Eq. (8) can be rewritten as

$$\gamma_r=\frac{2\hbar\omega^2e^2\epsilon_m^{1/2}N}{3mc^3}\left\{\left[\frac{\omega^2}{\omega_p^2}(1-\epsilon_m)-1\right]^2+\frac{1}{\omega^2\tau_{\rm nr}^2}\right\}, \tag{9}$$

where N is the number of free electrons in the particle, ω_p is the plasma frequency, and the nonradiative relaxation time $\tau_{\rm nr}$ equals $\hbar\gamma_{\rm nr}^{-1}$. Considering that $\tau_{\rm nr}^{-1}\ll\omega\ll\omega_p$, Eq. (9) can be simplified as

$$\gamma_r=\frac{2\hbar\omega^2e^2\epsilon_m^{1/2}N}{3mc^3}, \tag{10}$$

which indicates that the radiative relaxation rate is independent of temperature.

C. Relaxation by electron-surface scattering

The size of a metal nanoparticle is usually comparable to or smaller than the mean-free path of the conduction electrons, which adds another term to the plasmon relaxation due to the electron-surface scattering. This term can be calculated from a semiclassical relation,

$$\tau_S^{-1}=A\frac{v_FS}{4V}, \tag{11}$$

where v_F is the Fermi velocity, S and V are, respectively, the surface area and the volume of the nanoparticles, and A is a phenomenological factor.[24,25] Taking a typical gold bipyramid which has an equator radius of 15 nm, a total length of 85 nm, and a tip radius of 5 nm, and taking A to be 0.1 from previous measurements,[25] the electron-surface scattering $\gamma_S=\hbar\tau_S^{-1}$ is about 5 meV. This term is also independent of temperature. The sum of the electron-surface scattering rate and the radiative relaxation rate is thus expected to be 23 meV at all temperatures, which is in good agreement with the experimental results.

IV. CONCLUSION

In this paper, we have shown that plasmon relaxation in gold nanoparticles can be slowed by reducing the temperature of the particles. Overall, the plasmon linewidth in gold bipyramids is reduced by approximately 30% from room temperature to liquid-helium temperatures due to the reduction in electron-phonon scattering. At temperatures below about 50 K, the linewidth is nearly independent of temperature and is caused by radiative damping, electron-surface scattering, electron-electron scattering, and the temperature-

independent portion of electron-phonon scattering. Although the first two of these four mechanisms depend on the nanoparticle shape and size, and can thus potentially be reduced further, the electron-electron scattering and electron-phonon scattering are characteristics of gold. This means that the plasmon damping rate in gold nanoparticles is limited to be at least 43 meV regardless of particle geometry or temperature. This intrinsic damping is expected to be lower in silver nanoparticles—approximately 26 meV according to Eqs. (5)–(7) and experimental data for bulk silver[10,21]—but still sets a fundamental limit on plasmon lifetimes in the near-IR spectral range. The same mechanisms will ultimately limit propagation lengths of surface-plasmon polaritons on metal films and in plasmonic waveguides.

ACKNOWLEDGMENTS

M.L. was supported by the University of Chicago MRSEC NSF-DMR under Grant No. DMR-0213745. Partial support from NSF under Grant No. NSF-CHE-0718718 is also acknowledged. Work at the Center for Nanoscale Materials was supported by the Office of Science, Office of Basic Energy Sciences, U.S. Department of Energy under Contract No. DE-AC02-06CH11357. M.L. also thanks Praket P. Jha for his help with the low-temperature measurements.

*Present address: Department of Chemistry and Chemical Biology, Harvard University, Cambridge, Massachusetts 02143. liu13@fas.harvard.edu

†pgs@uchicago.edu

[1] S. A. Maier, M. L. Brongersma, P. G. Kik, S. Meltzer, A. A. G. Requicha, and H. A. Atwater, Adv. Mater. **13**, 1501 (2001).

[2] P. Anger, P. Bharadwaj, and L. Novotny, Phys. Rev. Lett. **96**, 113002 (2006).

[3] S. Kühn, U. Håkanson, L. Rogobete, and V. Sandoghdar, Phys. Rev. Lett. **97**, 017402 (2006).

[4] S. A. Maier, P. G. Kik, H. A. Atwater, S. Meltzer, E. Harel, B. E. Koel, and A. A. G. Requicha, Nature Mater. **2**, 229 (2003).

[5] V. M. Shalaev, Nat. Photonics **1**, 41 (2007).

[6] H. J. Lezec, J. A. Dionne, and H. A. Atwater, Science **316**, 430 (2007).

[7] K. A. Willets and R. P. Van Duyne, Annu. Rev. Phys. Chem. **58**, 267 (2007).

[8] C. Sönnichsen, T. Franzl, T. Wilk, G. von Plessen, J. Feldmann, O. Wilson, and P. Mulvaney, Phys. Rev. Lett. **88**, 077402 (2002).

[9] C. Kittel, *Introduction to Solid State Physics*, 6th ed. (Wiley, New York, 1986).

[10] J. A. Mckay and J. A. Rayne, Phys. Rev. B **13**, 673 (1976).

[11] F. Wang and Y. R. Shen, Phys. Rev. Lett. **97**, 206806 (2006).

[12] U. Kreibig, J. Phys. F: Met. Phys. **4**, 999 (1974).

[13] M. Z. Liu and P. Guyot-Sionnest, J. Phys. Chem. B **109**, 22192 (2005).

[14] A. Gole and C. J. Murphy, Chem. Mater. **17**, 1325 (2005).

[15] U. Kreibig and M. Vollmer, *Optical Properties of Metal Clusters* (Springer, New York, 1995), pp. 317-321.

[16] M. Z. Liu, P. Guyot-Sionnest, T.-W. Lee, and S. K. Gray, Phys. Rev. B **76**, 235428 (2007).

[17] C. F. Bohren and D. R. Huffman, *Absorption and Scattering of Light by Small Particles* (Wiley, New York, 1983), pp. 141–151.

[18] J. J. Olivero and R. L. Longbothum, J. Quant. Spectrosc. Radiat. Transf. **17**, 233 (1977).

[19] R. N. Gurzhi, Sov. Phys. JETP **8**, 673 (1959).

[20] W. E. Lawrence and J. W. Wilkins, Phys. Rev. B **7**, 2317 (1973).

[21] G. R. Parkins, W. E. Lawrence, and R. W. Christy, Phys. Rev. B **23**, 6408 (1981).

[22] R. N. Gurzhi, Sov. Phys. JETP **6**, 506 (1958).

[23] T. Holstein, Ann. Phys. (N.Y.) **29**, 410 (1964).

[24] E. A. Coronado and G. C. Schatz, J. Chem. Phys. **119**, 3926 (2003).

[25] M. Z. Liu and P. Guyot-Sionnest, J. Phys. Chem. B **108**, 5882 (2004).